

## An Evolution-Based Approach to De Novo Protein Design

Jeffrey R. Brender, David Shultis, Naureen Aslam Khattak,  
and Yang Zhang

### Abstract

EvoDesign is a computational algorithm that allows the rapid creation of new protein sequences that are compatible with specific protein structures. As such, it can be used to optimize protein stability, to resculpt the protein surface to eliminate undesired protein-protein interactions, and to optimize protein-protein binding. A major distinguishing feature of EvoDesign in comparison to other protein design programs is the use of evolutionary information in the design process to guide the sequence search toward native-like sequences known to adopt structurally similar folds as the target. The observed frequencies of amino acids in specific positions in the structure in the form of structural profiles collected from proteins with similar folds and complexes with similar interfaces can implicitly capture many subtle effects that are essential for correct folding and protein-binding interactions. As a result of the inclusion of evolutionary information, the sequences designed by EvoDesign have native-like folding and binding properties not seen by other physics-based design methods. In this chapter, we describe how EvoDesign can be used to redesign proteins with a focus on the computational and experimental procedures that can be used to validate the designs.

**Key words** Protein design, Evolutionary profile, Protein structure modeling, Experimental protein validation, Recombinant expression, Circular dichroism, Nuclear magnetic resonance

---

## 1 Introduction

Computational protein design has expanded in recent years from the prediction of the effects of single site mutations to the complete redesign of entire proteins, including the alteration of protein-protein binding affinity and specificity [1–4], enzymatic activity [5, 6], and even the creation of new folds [7] and functions [8] that are not seen in nature. On the theoretical side, protein design has been used to find the sequence constraints necessary to generate specific folds or functions [9–11]. Through the use of these constraints, fundamental questions in protein evolution have been addressed by distinguishing what is physically possible from what is actually observed in evolution [10, 12].

However, full protein redesign beyond the mutation of a few hot spot residues, called *de novo* design, is computationally difficult,

which is reflected in the relatively low successful percentage of 34  
successful designs. Most algorithms for de novo protein design 35  
approach the problem as reverse ab initio protein folding, evaluat- 36  
ing the energy of the sequence according to all-atom physical 37  
potentials. Several problems become apparent in the naïve applica- 38  
tion of this approach: (1) A very large number of sequences must be 39  
considered, which limits the force field to only approximate energy 40  
terms that can be rapidly calculated; (2) there is a mismatch 41  
between the low-resolution models generated in the sequence 42  
search and the all-atom physical potentials used for evaluation. To 43  
make the design simulation computationally tractable, the possible 44  
conformations of the side-chains of the protein are restricted to a 45  
limited set of discrete rotamer conformations. The small steric 46  
clashes that necessarily result from this approximation force the 47  
use of dampened potentials that may miss subtle interactions that 48  
exist in the native protein [13, 14]; (3) the sequence search is 49  
considered only with the protein in isolation, not as the protein 50  
actually exists in the cellular context. This causes subtle problems in 51  
the real-life application of the designed proteins, particularly with 52  
respect to aggregation, as the highly hydrophobic sequences 53  
favored by folding energetics generally adopt highly compact 54  
sequences in silico but tend to aggregate in reality when actually 55  
expressed [15]. 56

One approach to handle these challenges is to increase the 57  
accuracy of the design process by attempting to model physical 58  
reality at a higher resolution. In this spirit, design methodologies 59  
have been created that explicitly consider multiple conformations 60  
of the folded protein using ensemble techniques for multistate 61  
design [16–18] or that explicitly consider the unfolded state during 62  
the design process [18]. Alternatively, other design methodologies 63  
have been created that recognize the inherent inaccuracy of the 64  
force fields and attempt to diminish the effects of known inaccura- 65  
cies. One example is the use of soft-core potentials that lessen 66  
repulsive interactions, preventing strongly unfavorable interactions 67  
that can be alleviated by small backbone motions from overriding 68  
the other terms [19]. Another example of this approach is the 69  
inclusion of additional terms in the force field that consider factors 70  
relevant to real proteins that are missing in the simulation, for 71  
example, the explicit consideration of inappropriate hydrophobic 72  
surfaces to limit aggregation in the designed sequences [18, 20]. 73  
The ongoing development of these methods has contributed 74  
greatly to the field and has led to some spectacular successes. 75  
However, complete de novo protein design is still a difficult process 76  
with routine application still in the future. 77

An alternative approach, based on hard-won knowledge from 78  
protein fold-recognition and structure prediction [21–24], is to 79  
recognize that evolution implicitly encodes information on protein 80  
folds and binding interactions that greatly exceeds our ability to 81

describe it through reductionist, physics-based methods. This evolution-based method approach to protein design differs from the physics-based methods in that most energy terms are not dependent on the full-atom representation of each tested sequence, whose inaccuracy is a significant source of error. Instead, the sequence space search is constrained by the sequence and structural profiles collected from structurally analogous families, assisted by neural network predictions of local structural features, including secondary structure, backbone torsion angle, and solvation [25, 26].

## 2 Methods

### 2.1 *EvoDesign: Evolution-Based Method to Design Protein Folds and Interactions*

The principle of *EvoDesign* follows the critical lessons learned from threading-based protein structure prediction methods, i.e., to use the reliable “finger-print” of nature of multiple proteins from the same family in the form of structural profile information to guide the simulation to the sequence search. It first collects a set of proteins with similar folds to the target scaffold structure from the PDB library by the structural alignment program TM-align [27], using a TM-score cutoff value to define structural similarity (Fig. 1) [28]. In the second step, this set of structurally similar folds is used to create a position specific scoring matrix  $M(p, a)$  for evaluating potential sequences [29, 30].

To create the position specific scoring matrix, first a multiple sequence alignment (MSA) is generated according to the pair-wise structural alignments between the structural analogs identified in the first step and the target structure (Fig. 1). An  $L \times 20$  matrix (where  $L$  = length of the protein) is then created according to

$$M(p, a) = \sum_{x=1}^{20} w(p, x) \times B(a, x) \quad (1)$$

where  $x$  represents a particular amino acid,  $B(a, x)$  is the BLO-SUM62 substitution matrix [31] for amino acid  $x$  to amino acid  $a$ , and  $w(p, x)$  is the frequency of the amino acid  $x$  appearing at position  $p$  in the MSA created by TM-align. The matrix  $M(p, a)$  serves as a structural profile to guide the sequences toward native-like sequences known to adopt structurally similar folds as the target (Fig. 1).

While the structural profile as given by the position specific scoring matrix  $M(p, a)$  is efficient in guiding the global fold, optimization on the profile alone can result in singularities (i.e., disjointed “islands”) in local sequences. To smoothen these singularities, back propagation neural network predictors are used to estimate the secondary structure (SS), solvent accessibility (SA), and torsion angles ( $\varphi/\psi$ ) of the sequence. Unlike other predictors for these

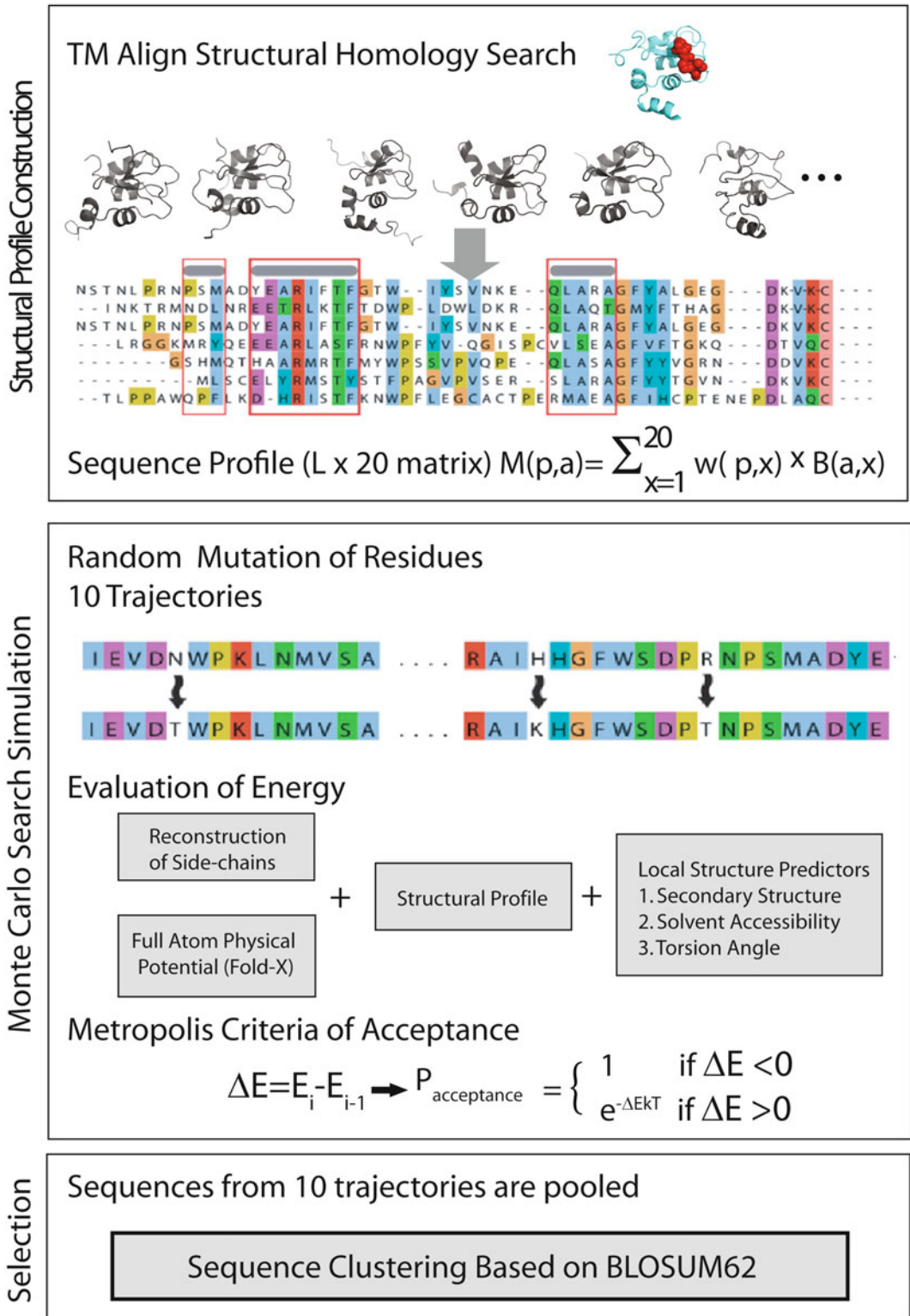


**Fig. 1** Overview of the EvoDesign method showing the construction of the structural profile, the Monte Carlo search in sequence space, and the final selection of the sequences by sequence clustering

properties [32–34], these single-sequence-based predictors do not require a computationally expensive PSI-BLAST search, which considerably speeds up prediction at little cost in accuracy [25].

The evolutionary potential in EvoDesign is defined as the maximum score of the optimal alignment path between the decoy and target structure obtained by Needleman-Wunsch dynamic programming, giving the energy function:

$$E_{\text{evolution}} = \sum_{\text{max}} [M(p, a) + w_1 \Delta SS(p) + w_2 \Delta SA(p) + w_3 (\Delta \varphi(p) + \Delta \psi(p))], \quad (2)$$

where  $\Delta SS$ ,  $\Delta SA$ ,  $\Delta \varphi$ , and  $\Delta \psi$  are the difference in secondary structure, solvent accessibility and torsion angles between the target assignments, and the predictions from the decoy sequences. The weighting factors ( $w_i$ ) are decided by the relative accuracy of the single-sequence-based predictions for each term on a training set [25].

A physics-based potential can be used to predict potential favorable and unfavorable interactions among side-chains, such as steric interactions, which may be missed by the evolutionary-based terms defined above. While our computational benchmark results indicate the evolution-based energy function alone is sufficient to design protein sequences, adding a physics-based energy term from FoldX [35] improved the atomic packing of the local structures based on both computational structure prediction and experimental structure validations [25]. In this case, a full-atom representation of the sequence is needed which is created by SCWRL [36].

The final force field for single-chain protein design in EvoDesign is given by the weighted Z-scores of the evolution and physics-based terms:

$$E = w_4 \frac{E_{\text{evolution}} - \langle E_{\text{evolution}} \rangle}{\delta E_{\text{evolution}}} + w_5 \frac{E_{\text{foldX}} - \langle E_{\text{foldX}} \rangle}{\delta E_{\text{foldX}}}, \quad (3)$$

where  $\langle \dots \rangle$  and  $\delta$  indicate the average and standard deviation of the energy terms.

To actually generate the designed sequences, Monte Carlo searches are performed starting from 10 random sequences that are updated by random residue mutations (Fig. 1). Due to the imprecision of the force field, the lowest energy states do not always correspond to the best sequence design. Instead of simply focusing on the lowest energy sequence, the sequences from all 10 runs are pooled and the sequence with the maximum number of neighbors is identified using the SPICKER clustering algorithm [37] where the pair-wise distance between sequences is measured by the sum of the BLOSUM62 substitution scores [38].

The above procedure finds sequences compatible with the target structure. To introduce new or altered functionality into

the protein, the affinity of existing protein-protein interfaces can be improved by EvoDesign or new interfaces created through the optimization of non-native complexes created by docking. To modify interfaces, EvoDesign uses a multiscale approach incorporating a variety of features at different levels of structural resolution (Fig. 2).

Similar to the design of protein folds with EvoDesign, a key feature of the binding potential is the mixture of physics-based and evolutionary terms in the energy function [39]. For interface modification, the evolutionary terms are created from the structural alignment of similar interfaces from the nonredundant COTH structural library of dimeric proteins [40] by the IAlign program

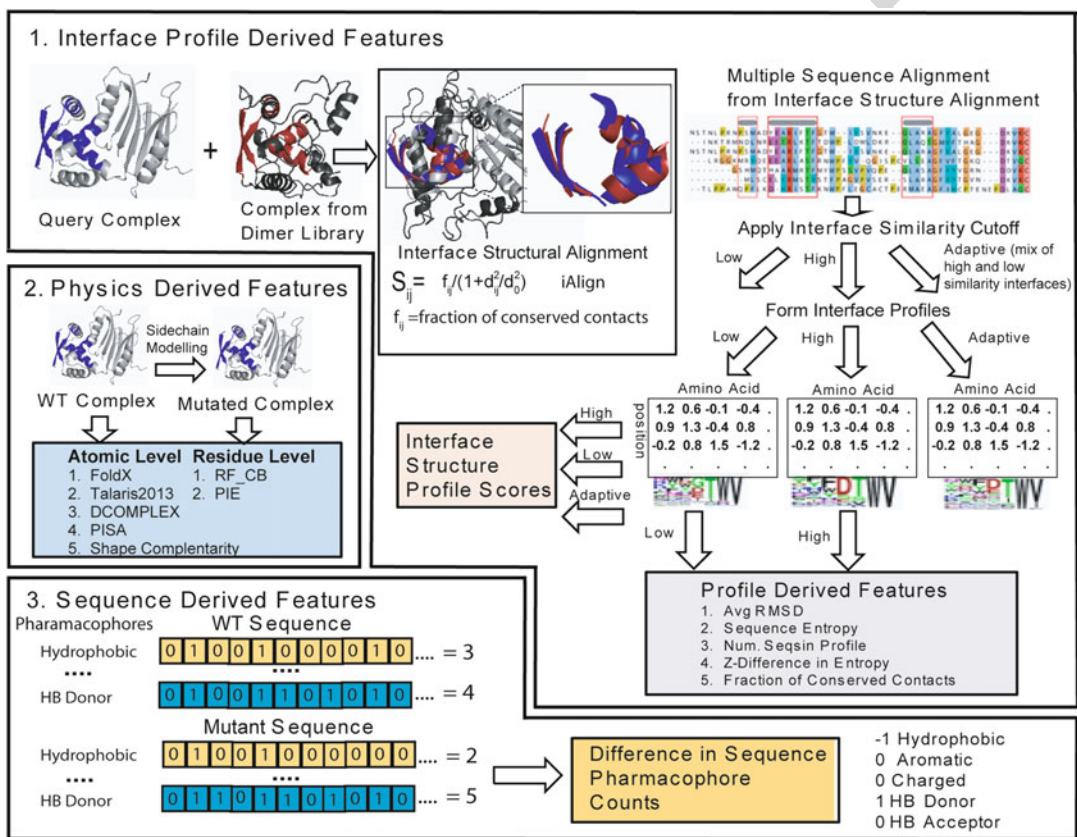


**Fig. 2** Multiscale approach to predicting protein binding affinity using features derived from interface structural profiles, WT and mutant sequences, and physics-based scoring of the structures of the wild-type and mutant complexes. (1) Interface profile scores derived by structural alignment of structurally similar interfaces using an interface similarity cutoff to define the aligned sequences that are used to build the profile. (2) Physics-based scores are formed at the residue or atomic level formed by modeling the mutant monomeric protein and complex and evaluating the difference in energy. (3) Sequence features are formed by the difference between the WT and mutant sequences in the number of hydrophobic (V, I, L, M, F, W, or C), aromatic (Y, F, or W), charged (R, K, D, or E), hydrogen bond acceptors (D, E, N, H, Q, S, T, or Y), and hydrogen bond donating residues (R, K, W, N, Q, H, S, T, or Y) along with difference in amino acid volume calculated from the sequence

[41]. A series of interface similarity cutoffs has been used to define three separate interface structure profiles along with different metrics designed to assess the accuracy of the profiles relative to the other terms [39]. The interface profiles scores are then combined with physics-based all-atom and residue level docking scores. Finally, sequence-based scores based on pharmacophore count differences between the native and designed sequences are calculated to complete the multiscale approach. A random forest method trained to predict the experimental affinity changes ( $\Delta\Delta G$ ) associated with single and multiple mutations at the interface is used for the final interface energy score. This energy score has a correlation to the experimental  $\Delta\Delta G$  values equivalent or superior to the best state-of-the-art mutation prediction programs (Pearson's correlation coefficient = 0.83 for a 5 fold cross validated set) but is fast enough to calculate the thousands of potential mutations necessary for protein design. The interface energy is then added to the regular EvoDesign scoring potential, using a user-defined weighting function to balance fold stability and protein-protein affinity.

## 2.2 Using the EvoDesign Server Design Program

The EvoDesign program can be used as a server at <http://zhanglab.ccmb.med.umich.edu/EvoDesign>. The only input to the server is a PDB format file of the target structure, which can be either a full-atomic or backbone only model. In either case, the backbone of the protein structure should be complete without breaks in the chain. Currently, the server is limited to design of one protein chain only.

There are three user-defined parameters to control the design simulation. The first parameter is the fold-similarity cutoff used for defining the structural profile (Eq. 1). By default, this is set to the relatively high value of a TM score of 0.7, which is relaxed if less than ten structural analogues are found in the PDB. This value can be adjusted to a higher or lower value; lower values incorporate more sequence and structural variability in constructing the profile while higher values incorporate less. The usual result is that higher cutoffs penalize deviations from the native sequence more strongly, which may or may not be desirable for the particular application. The second parameter controls whether the FoldX force field is used in the simulation or not. Inclusion of FoldX usually results in only a marginal improvement in the folding when validated by structure prediction (see the next section) [25], most likely due to the fact that the side-chains are modeled by a different force field from the SCWRL force field used for scoring. Including FoldX in the simulation requires that the full atomic model of each sequence be constructed, which is the most computationally demanding step in the simulation. For this reason, the FoldX force field is turned off by default. The last parameter does not affect the design simulation but controls whether structure prediction is performed for each of the designed sequences through the creation of I-TASSER models (*see* Subheading 2.3.1).

By default, the EvoDesign server operates without any residue restrictions on the design process. In many cases, it is desirable to freeze certain residues in the design process, such as those involved in disulfide bond formation or in ligand binding. Taken further, in other cases, it is useful to redesign only the surface of the protein while keeping the inner core constant. An option is therefore provided to specify a set of residues (by residue number) which should be kept the same as in the input structure. It is also sometimes desirable to restrict the use of some residues completely or at certain positions. A prime example is cysteine residues on the surface, which can easily be oxidized to form intermolecular disulfide bonds that lead to a loss of activity through aggregation.

The output of the server is ten sequences in decreasing order of cluster size from the clusters generated by the SPICKER algorithm. For each sequence, the sequence identity to the native sequence is calculated along with the predicted normalized relative error for the secondary structure, solvent accessibility, and torsion angles. Each property is calculated by a high accuracy predictor using PSI-BLAST profiles along with neural network predictors (PSSPred for secondary structure prediction [42], ANGLOR for torsion angle prediction [32], and the method of SOLVE for solvent accessibility [43], respectively). The normalized relative error (NRE) is reported for each prediction, which is defined by [25].

$$NRE = \frac{EDS - ETS}{ETS}, \quad (4)$$

where *EDS* refers to “error of designed sequence,” i.e., the mismatch between the predicted structure feature from the designed sequence and the target structure. *ETS* refers to “error of target sequence” that is defined similarly to *EDS* but for the target sequence. The *NRE* defined thus accounts for the uncertainty from the structure feature predictors. Finally, I-TASSER models of each of the designed sequences are provided if user selects the third option on I-TASSER modeling. The I-TASSER models represent a partial validation of the success of the design simulation as described below.

### 2.3 Computational Validation of Protein Designs

No computational design method is perfect, and validation remains an essential part of the design processes. Validating experimentally that the designed protein sequence successfully folds to the desired structure requires both successfully expressing the protein and successfully determining the structure. A full structure determination at the atomic level through either NMR spectroscopy or X-ray crystallography is a time-consuming and difficult task. Even simpler, less precise experimental methods for determining protein structure, such as comparing the secondary structure of the native and designed proteins through circular dichroism CD (*see*



Subheading 2.4.7) and recognition of the presence of folded tertiary structure through 1D NMR (*see* Subheading 2.4.8), still require that the protein be successfully expressed. Compared to computational techniques, protein expression is relatively expensive, limited in throughput, and in some cases may be challenging to achieve. Before expression, it is therefore desirable to know which designed sequences are most likely to fold to the target structure. The first step is to visually confirm that the design sequences are compatible with the structure. Specifically, it is a good idea to look for buried charges without salt-bridges and buried side-chains without hydrogen bonding partners before proceeding. The EvoDesign program uses a fixed backbone approximation in its calculations. High energies from van der Waals clashes can usually be relieved by small changes in the backbone [44, 45]. However, buried charges and missing hydrogen bonds are much harder to compensate for by small structural movements. Since even one missed hydrogen bond or buried charge is enough to completely destabilize a structure, any designs possessing these features should be eliminated from consideration.

It is, however, not possible to tell reliably if a protein will fold correctly by simple visual analysis. Accurate structure prediction of designed sequences is therefore central to the EvoDesign methodology, as it allows a much larger number and variety of sequences to be tested for correct folding than can be experimentally checked. EvoDesign currently employs I-TASSER, which is a hierarchical approach to protein structure modeling that constructs protein 3D models by reassembling continuous fragments excised from the multiple threading templates [43, 46–48]. I-TASSER has been extensively tested in both benchmarking [46, 47, 49] and blind tests [50–53]. In particular, the community-wide CASP (Critical Assessment of protein Structure Prediction) experiment is designed to benchmark the state-of-the-art of protein structure predictions every two years since 1994 [54–56]. I-TASSER was tested (as “Zhang-server”) in the 7–11th CASP competitions in 2006–2015. Figure 3 shows the histogram of the *Z*-score of the GDT-score, which measures the significance of the model predictions by each group of automated structure predictors compared to the average performance, in the latest 11th CASP competition. The data shows the advantage of the I-TASSER in comparison to other state-of-the-art protein structure prediction methods, provided that the protein is already known to fold to a specific structure.

### 2.3.1 Estimating Structural Fidelity and Foldability of Designed Sequences Using I-TASSER

The I-TASSER-based structure prediction of designed sequences in EvoDesign seeks to answer two related but distinct questions. First, does the designed sequence fold to any structure at all or is it only partially or completely unfolded when expressed? Second, given that the protein folds, does it fold to the correct structure? If a designed sequence is known to fold, there is considerable evidence

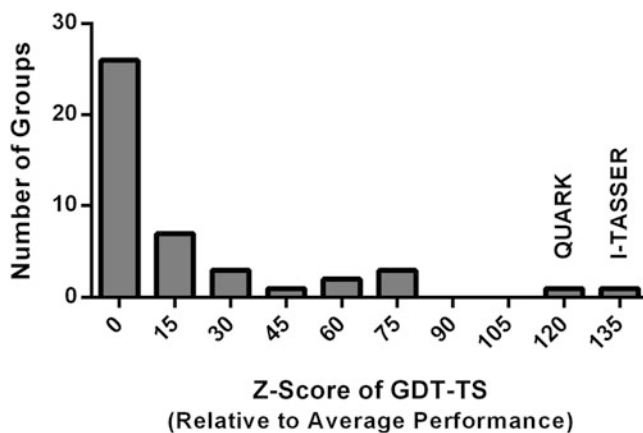


**Fig. 3** Histogram of the Z-scores of all automated protein structure predictors in the CASP11 experiment. The first bin contains groups that have Z-score below 0. Data are taken from official CASP webpage at URL [http://www.predictioncenter.org/casp11/zscores\\_final.cgi?model\\_type=first&gr\\_type=server\\_only](http://www.predictioncenter.org/casp11/zscores_final.cgi?model_type=first&gr_type=server_only)

from the benchmark and blind tests described above that I-TASSER could, with some confidence, tell if it will fold to its target structure. However, the ability of template-based protein structure programs to determine whether or not a given sequence can fold correctly to any structure at all has been tested much less extensively (*see Note 1*).

In an early test, I-TASSER was shown to cleanly distinguish native sequences from random sequences with similar sequence identity and secondary structural propensity [38]. For a more stringent benchmark test, we recently tested 16 successfully designed sequences that are known to match their target structure and 29 unsuccessful sequences that were known to either fold to a different structure or were unable to fold at all in the literature [25]. As shown in Fig. 4, I-TASSER successfully captured the deviation of the structures of the designed sequences from the target structure. Furthermore, the confidence level (*C*-score) [57] of the I-TASSER prediction is roughly correlated with the chance of success of the design: a *C*-score below  $-1.5$  indicates an almost certain failure and a *C*-score above 0 indicates a very strong possibility of success. I-TASSER prediction on designed sequences can therefore allow a winnowing out of poorly designed sequences without resorting to the lengthy procedure of expressing and experimentally determining the structures of designed proteins at each step.

#### 2.4 Experimental Validation of Designed Sequences

True validation of the designed protein requires that protein be characterized experimentally for structural fidelity and activity. The processes listed below have been employed in the EvoDesign

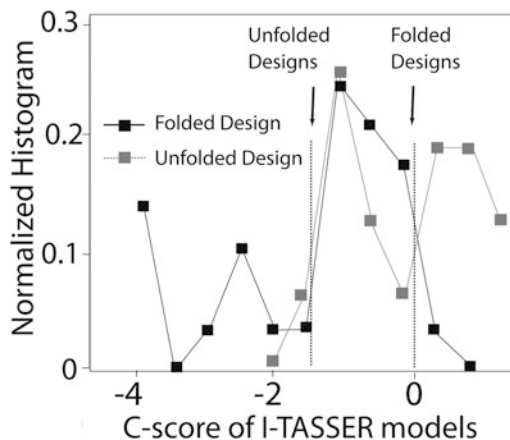


**Fig. 4** Divergence in the confidence score of the I-TASSER models for successfully and unsuccessfully designed sequences. Approximate cutoff values are indicated by the arrows. A  $C$ -score  $< -1.5$  indicates a high probability that the design will not be folded correctly and a  $C$ -score  $> 0$  indicates a high probability that the design will fold to the target structure

studies [25, 58], aiming to ensure that the designed proteins are thermodynamically stable, soluble, and adopt the desired fold. In all cases, the same tests should be performed with the wild-type protein as well for a control.

#### 2.4.1 Expression and Purification of Designed Proteins

Before a protein can be characterized experimentally, the pure protein must be generated in sufficient quantities for the experiments. This is done through a process called recombinant expression, which involves incorporating the DNA sequence of the designed protein into the genome of another organism and using that organism's protein production process to generate the target protein. Since there are many variations on the technique and the specifics of the process can vary with the protein being produced, a comprehensive description of the technique is not given here. Instead, key considerations are outlined in a basic manner for those unfamiliar with process. For further, more depth treatment readers are encouraged to consult several excellent reviews on this topic [59].

#### 2.4.2 Choice of Host Cell

The first decision that must be made in setting up a recombinant protein expression system is the choice of the host cell whose protein synthesis machinery will produce the target protein. This choice is one of the most critical ones as the choice of the expression organism defines the scope of the project, the reagents and equipment needed, and the final outcome of the expression process [59]. Each protein expression has advantages and disadvantages. In most cases, bacterial expression systems are favored as they are low cost,

easy to manipulate genetically, scale easily from small- to large-scale expression, and can easily incorporate isotopic labels for NMR studies. The main disadvantage of bacterial expression is that eukaryotic posttranslational modifications such as glycosylation and phosphorylation are not performed. In the case that these posttranslational modifications are essential, a eukaryotic host cell such as yeast or insect cells must usually be used and the process becomes considerably more complex.

Disulfide bond formation is also more difficult in bacteria, although this may be overcome in most cases by selecting a bacterial strain such as the Orgami cell line that have mutations in the thioredoxin reductase and glutathione reductase genes, which creates an oxidative environment that greatly enhances disulfide bond formation in the cytoplasm [60]. Expression can vary greatly for different bacterial strains. For this reason, different specialized strains of bacteria have been created to optimize the expression of recombinant proteins. Most specialized bacterial strains for expression start with the BL21 genetic background that is deficient in the Ion and ompT proteases that can lead to improper cleavage of the protein product. Other bacterial strains attempt to minimize the difference in codon usage between the natural codon usage of the bacteria and the codon usage required to express the protein.

Recombinant expression of proteins can lead to a high demand for specific tRNAs that are normally produced in only small amounts by the bacteria. Depletion of these low abundance tRNAs can cause translation to stall on the ribosome, leading to premature release from the ribosome and the generation of truncated versions of the protein [61]. From our studies [25, 58, 62], we recommend for routine use of the Rosetta 2 bacterial cell line that combines the protease mutations found in the BL21 strain along with additional modifications that allow the bacteria to generate low abundance tRNAs more efficiently and mutations that allow tunable expression through mutations in the Lac permease gene (see below). However, alternate strains may be considered in certain situations such as the Rosetta-gami strain, which adds the disulfide-bond promoting mutations of the Orgami strain to the Rosetta background.

#### 2.4.3 Selection of Expression Vector

Once the host cell is selected, the next step is to create the vector that introduces the foreign DNA into host cell. This is typically a bacterial plasmid that contains several elements besides the DNA encoding the target protein. The first element is a gene for antibiotic resistance which provides a growth selection mechanism for discovery; only those bacteria that have incorporated the plasmid into their genome can grow in the presence of the antibiotic. The second is the promoter system, which ties the expression of the target protein to another protein whose expression is essential for

the cell and whose expression can be readily induced at a specific 417  
 time. Triggering expression at a specific time is essential as bacteria 418  
 continue to grow during incubation and the time at which the 419  
 protein is lysed determines the overall yield and final purity of the 420  
 product. If the cell density is too low, the yield of expressed protein 421  
 is naturally low. On the other hand, too high of cell density can also 422  
 result in decreased yields and purity from loss of the plasmid from 423  
 the bacteria [63], metabolism of the antibiotic within the medium, 424  
 and death of the bacteria from lack of dissolved oxygen [64]. 425  
 Typically, this is done through the use of the Lac operon, in 426  
 which protein expression can be induced at a specific time period 427  
 during growth with the lactose analog isopropyl  $\beta$ -D-1-thiogalacto- 428  
 pyranoside (IPTG). 429

#### 2.4.4 Purification of Expressed Protein

Once expressed, the expressed protein still needs to be purified 431  
 from the other proteins in the bacterial cell. Although this may be 432  
 accomplished using the sequence of the designed protein without 433  
 modification using multiple steps of column chromatography, it is 434  
 easier to fuse the designed sequence to other protein domains to 435  
 make purification easier. In many cases, the expressed protein is not 436  
 soluble at the very high concentrations generated during expres- 437  
 sion. In this situation, the expressed protein accumulates in an 438  
 insoluble form in the bacteria as particles known as inclusion bod- 439  
 ies. The formation of inclusion bodies can make purification easier 440  
 or more difficult. The inclusion bodies generally contain the 441  
 expressed protein in highly pure form with only a small amount 442  
 of the other proteins of the host cell mixed in, a clear advantage for 443  
 the purification process. On the other hand, proteins within inclu- 444  
 sion bodies must be first disaggregated and then refolded with urea, 445  
 which may prove a difficult process [65]. If the stability of the 446  
 protein is unknown, such as the case with designed proteins, it is 447  
 often easier to try to purify already folded, soluble proteins. 448

To enhance the solubility of proteins during purification, a 449  
 solubility tag such as the Mocr domain [66] can be fused to the 450  
 target protein. This domain is usually fused N-terminal to the 451  
 designed sequence. Since it is localized to the N-terminus, the 452  
 Mocr domain is therefore synthesized first and folds into its native 453  
 form before the translation of the designed sequence, stabilizing 454  
 the designed domain's folding process. Moreover, the high nega- 455  
 tive charge on the Mocr domain increases the solubility during the 456  
 purification process by preventing self-association by electrostatic 457  
 repulsion. Along with the solubility tag, another sequence that 458  
 specifically binds a particular column can be incorporated to assist 459  
 purification. A common choice is the His tag, six consecutive 460  
 histidine residues that strongly bind nickel (Ni) columns. A prote- 461  
 ase cleavage site is often placed between the Mocr domain with the 462  
 His tag and the sequence of the designed protein so that the two 463

domains can be separated. The expressed protein with the Mocr/His tag will bind the Ni column; most other bacterial proteins will not. The Mocr/His domain is then cleaved from the target sequence by the addition of a protease specific to the cleavage site and passed through the Ni column again. This time, the target protein does not bind the Ni column but all other nickel-binding proteins will remain bound to the column. The end result of this process is a highly pure protein in a soluble form.

#### 2.4.5 Confirmation of Protein Solubility

In addition to adopting a stable folded conformation, many proteins must be soluble in water to perform their biological function. This requirement constrains the design process, as sequences that are optimized only for stability of the folded conformation may not be optimized for solubility. A key advantage of the EvoDesign method is that the structural profiles implicitly include all the constraints involved in determining the sequences that are compatible with a specific fold, not just those concerned with fold stability. As a result, sequences designed by EvoDesign are significantly more native-like in composition than those designed by physics only methods [25], which tend to overemphasize hydrophobic residues on the surface more than is found in native proteins [20, 38, 67]. Consequently, aggregation by the coalescence of exposed hydrophobic patches is a common source of failure in physics-based design [20].

As aggregation generally makes a protein useless for most applications, the oligomeric state of the protein should be determined before proceeding at the highest concentration used for the other biophysical experiments. Typically, this is around 100  $\mu\text{M}$  for a 100-residue domain. The limiting factor is usually sensitivity of the 1D NMR experiment for tertiary structure estimation and sensitivity of the urea denaturation experiment used for the determination of protein stability (*see Note 2*). An approximate concentration range may be established by measuring the signal-to-noise ratio at different concentrations of the native protein. The signal of both experiments is actually more sensitive to the total concentration by weight than the molar concentration. The 100  $\mu\text{M}$  value may need to be adjusted upward or downward for proteins significantly shorter or longer than 100 residues.

The presence of aggregation is most readily determined quantitatively by dynamic light scattering, which measures the hydrodynamic radius of proteins in solution, or from a correctly calibrated analytical size exclusion column. In the absence of either instrument, aggregation may be measured semiquantitatively by the absorbance at 400 nm. At this wavelength range, the protein does not absorb light and increases in absorbance are due to Rayleigh scattering, which is proportional to the sixth power of the particle radius. A comparison to the corresponding absorbance at 400 nm

- of the native protein provides a qualitative estimate of the amount of aggregation in the sample (*see* **Note 3**).
- 2.4.6 Confirmation of Structural Fidelity** X-ray crystallography remains the gold standard for confirming whether a protein design has the desired structure. However, not all well-folded proteins crystallize and the expense of X-ray crystallography severely restricts the number of designs that can be studied. From a functional perspective, absolute structural fidelity is not necessary in many cases and small changes on the atomic scale are tolerated if the protein is stable, soluble, and functional. To test a larger number of sequences, faster low-resolution biophysical techniques can be used to eliminate obviously badly designed sequences [68, 69].
- 2.4.7 Confirmation of Secondary Structure** Secondary structure is the most basic building block of protein structure. The existence of severely incorrect secondary structure in the designed protein therefore very strongly implicates a failed design. Since each secondary structure element ( $\alpha$ -helix,  $\beta$ -sheet, and random coil) has a distinct circular dichroism (CD) spectra, the relative fractions of each in a protein can be estimated from a CD spectra by fitting to a reference set of proteins with known CD spectra and secondary structure [70]. The accuracy of this procedure is typically around  $\pm 5\%$ , with  $\alpha$ -helical content determined more precisely than either random coil or beta sheet content. If available, infrared (IR) spectra can also be used in a similar manner to characterize the secondary structure, as it has been shown that IR and CD are largely complementary and a combination of the two techniques gives a more accurate picture of the secondary structure than either technique alone [71].
- 2.4.8 Confirmation of Existence of Tertiary Structure** The existence of tertiary structure has traditionally been defined in a qualitative way from the appearance of the 1D  $^1\text{H}$  NMR spectra of the protein. A protein that is poorly folded, without extensive contacts within the protein core, has a distinctive 1D NMR spectra characterized by the lack of highly shielded peaks in the region of the spectra from  $-1$  to  $0.5$  ppm and poor dispersion of the signal within the amide region (*see* Fig. 5) [72, 73]. While this method is standard in the protein design field [68, 69], it is subjective and qualitative. A more objective and quantitative method is to use the autocorrelation of a 1D  $^1\text{H}$  [74] or unassigned 3D  $^{15}\text{N}$  NOESY-HSQC NMR spectrum [75], which have been shown to accurately distinguish folded and unfolded proteins. A comparison of the binding of the dye SYPRO Orange, which binds to exposed hydrophobic surfaces, to the native sequence can provide an additional test for a misfolded protein structure [76].
- 2.4.9 Confirmation of Fold Stability** The free energy of folding can be measured using chemical denaturation with urea, with denaturation measured by the decrease in secondary structure as determined by CD [25]. As the

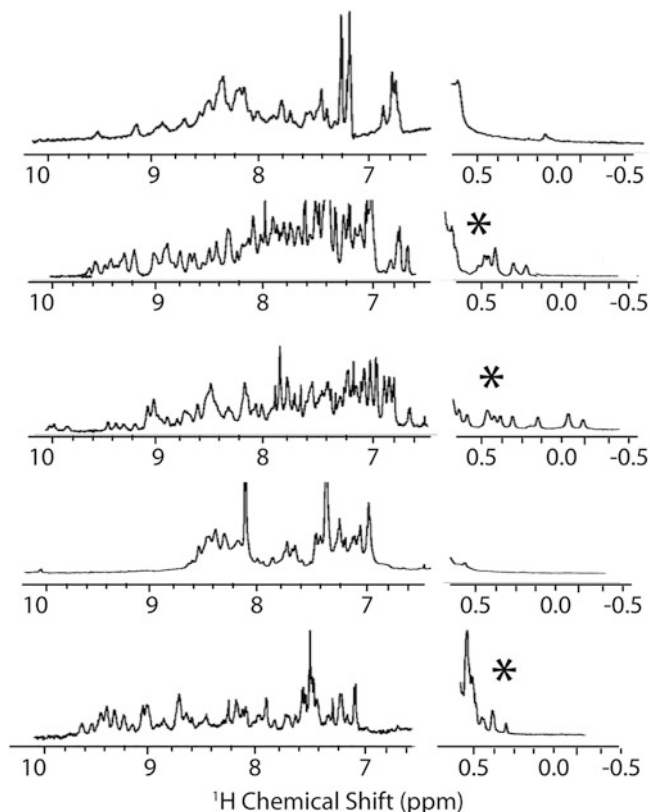


**Fig. 5** NMR spectra of folded (with *asterisk*) and unfolded designed proteins. The folded designs have a wider range of chemical shift values in the amide region of the spectrum (7–10 ppm) and have chemical shift values below 0.5 ppm indicating side-chains strongly shielded from solvent, as would be expected in a well-packed protein core

concentration of urea is increased, the protein unfolds, in most cases by a two-step process without a significant population of partially unfolded intermediates. The first step of determining the stability is to measure the CD signal without denaturant ( $CD_{\text{folded}}$ ), where it is assumed to be completely folded, and at a high concentration of denaturant, where it is assumed to be completely unfolded ( $CD_{\text{unfolded}}$ ). If unfolding is a two-step process, the CD signal as a function of the urea concentration is [77]:

$$CD(\text{urea}) = f_{\text{unfolded}}(\text{urea})CD_{\text{unfolded}} + f_{\text{folded}}(\text{urea})CD_{\text{folded}}, \quad (5)$$

where  $f_{\text{folded}}(\text{urea})$  and  $f_{\text{unfolded}}(\text{urea})$  refer to the fractions of folded and unfolded proteins respectively, at a given urea concentration. Since the equilibrium constant can be calculated directly from fraction of folded and unfolded proteins, the Gibbs free



energy of unfolding can be calculated for each urea concentration [77]:

$$K(\text{urea}) = \frac{f_{\text{unfolded}}(\text{urea})}{1 - f_{\text{unfolded}}(\text{urea})} \quad (6)$$

$$\Delta G(\text{urea}) = -RT \ln K(\text{urea}) = -RT \ln \left( \frac{f_{\text{unfolded}}(\text{urea})}{1 - f_{\text{unfolded}}(\text{urea})} \right) \quad (7)$$

The relevant free energy is the free energy of unfolding in the absence of denaturant, which can be obtained by linear extrapolation of the free energy to zero urea concentration.

---

### 3 Conclusions

Using an evolution-based approach, we have successfully designed, expressed, and experimentally characterized a number of single domain proteins [25, 58]. In the first benchmark test, we used EvoDesign to redesign 87 globular proteins randomly collected from the PISCES server. I-TASSER was then used to test the fidelity of the predicted structure to the target. Although all homologous templates have been excluded from the I-TASSER template library, out of the 87 designed sequences, 80 % were predicted to fold to structure with an RMSD of <2.0 Å to the target scaffold, and 42.5 % were predicted to fold to an essentially identical structure with an RMSD < 1.0 Å. This was a clear difference from designed sequences created using only the FoldX force field, for which only 54 % of the predicted structures have an RMSD < 2.0 Å to the target structure, and only 31 % have an RMSD < 1.0 Å.

In a separate test, we redesigned five globular proteins by EvoDesign and used the experimental validation procedures described in Subheading 2.4 to confirm the success of the designs. All five proteins were successfully expressed using the expression system in Subheading 2.4.3 and were soluble to at least 70 μM. Further, all five designed proteins have secondary structure consistent with the target protein (<12 % difference). Three out of the five had a compact tertiary structure confirmed by NMR (Subheading 2.4.8, Fig. 5), for an overall success rate of 60 %. One of the three, the Phox homology domain of the cytokine-independent survival kinase (CISK-PX), could be crystallized and its structure compared to the native protein [78]. Despite having only 32 % sequence identity, the structure of the designed protein showed a very close similarity to the target with a RMSD of 1.54 Å and a TM score of 0.90 to the target template. The RMSD and TM score between the I-TASSER model and the X-ray crystal structure of

CISK-PX are 1.32 Å and 0.91, respectively. Most of the difference between the two structures was in a loop that is disordered in the original structure.

Finally, we have shown that EvoDesign can be used to create functional complexes for the X-linked inhibitor of apoptosis proteins (XIAP) with improved properties by designing a peptide-protein complex involved in apoptosis inhibition [58]. The XIAP protein inhibits apoptosis by binding caspase-9, an activity that is in turn regulated by the second mitochondria-derived activator of caspases (SMAC). The designed XIAP protein by EvoDesign binds SMAC but does not possess affinity for caspase-9. As such, the designed protein can serve as a SMAC sink, altering the normal protein-protein interaction network involved in cell death. The circular dichroism and isothermal calorimetry data showed that the designed XIAP domain was more stable than WT-XIAP and bound the SMAC derived peptide with a  $K_d$  of  $167 \pm 67$  nM, which compares favorably with the  $80 \pm 25$  nM  $K_d$  found for WT-XIAP. Interestingly, a designed version of XIAP with native interface residues actually showed worse binding ( $K_d$  of  $352 \pm 79$  nM) and stability than the fully designed sequence, highlighting the efficiency of evolution-based full protein design.

---

## 4 Notes

1. The distinction between these two questions becomes clear when the nature of the benchmarks is considered. Due to the experimental requirements of structure determination, the benchmark test largely consists of proteins that can be successfully expressed, successfully purified, and are stable for a prolonged period of time at high concentration. In addition, the protein also must be crystallized in the case of X-ray structures, which is a rather severe restriction for proteins with large unfolded regions as the disordered regions have poor crystal contacts which interferes with the crystallization process [79]. Even if the protein can be crystallized, the disordered regions will have poor electron density and will therefore not be resolved in the structure. Similarly, the structure of unfolded proteins is difficult to determine by NMR due to the lack of long-range NOE constraints and poor chemical shift dispersion [80]. These experimental constraints suggest that though the PDB library is largely complete with respect to the possible universe of monomeric folded domains [81, 82], it is still biased toward compact folded structures, as proteins that are intrinsically unstable or unfolded are difficult to observe. The PDB library should therefore not be considered as completely representative of the conformational ensembles, folded or not, that all protein sequences can adopt.

2. The signal-to-noise ratio in an NMR experiment depends on a number of factors including the field strength of the NMR spectrometer (higher magnetic fields give higher resolution spectra and hence higher signal-to-noise ratios), the size of the protein (larger proteins give rise to broader signals), and other factors such as conformational exchange (transitions between conformations under certain timescales give rise broader signals). The signal-to-noise ratio in a CD spectrum also depends on a variety of factors, including the transparency of the buffer in the far UV region of the spectrum (180–260 nm), the path-length of the cuvette, and the age of the xenon lamp used to acquire the spectrum. Of these factors, the transparency of the buffer usually has the most impact. A buffer strongly absorbing in the UV serves as an inner filter that attenuates the incoming light reaching the protein. Phosphate buffers are optimal for CD due to their transparency in the far UV region of the spectrum, although Tris buffers are nearly as good. Chloride ions absorb in this region and the proteins in NaCl solutions should be dialyzed against an equivalent of concentration of NaF. Finally, many additives used to stabilize proteins, such as glycerol, arginine, and Triton-X, absorb strongly in the UV and are incompatible with CD spectroscopy for this reason.
3. An alternative wavelength can be used if the protein possesses a cofactor such as FAD or FMN that absorbs in the visible light range.

---

## Acknowledgment

The project is supported in part by the National Institute of General Medical Sciences (GM083107).

## References

1. Karanicolas J, Kuhlman B (2009) Computational design of affinity and specificity at protein-protein interfaces. *Curr Opin Struct Biol* 19(4):458–463
2. Kortemme T, Joachimiak LA, Bullock AN, Schuler AD, Stoddard BL, Baker D (2004) Computational redesign of protein-protein interaction specificity. *Nat Struct Mol Biol* 11(4):371–379
3. Shifman JM, Mayo SL (2003) Exploring the origins of binding specificity through the computational redesign of calmodulin. *Proc Natl Acad Sci U S A* 100(23):13274–13279
4. Lopes A, Busch MSA, Simonson T (2010) Computational design of protein-ligand binding: modifying the specificity of asparaginyl-tRNA synthetase. *J Comput Chem* 31(6):1273–1286
5. Procko E, Hedman R, Hamilton K, Seetharaman J, Fleishman SJ, Su M, Aramini J, Kornhaber G, Hunt JF, Tong L, Montelione GT, Baker D (2013) Computational design of a protein-based enzyme inhibitor. *J Mol Biol* 425(18):3563–3575
6. Jiang L, Althoff EA, Clemente FR, Doyle L, Rothlisberger D, Zanghellini A, Gallaher JL, Betker JL, Tanaka F, Barbas CF 3rd, Hilvert D, Houk KN, Stoddard BL, Baker D (2008) De novo computational design of retro-aldol enzymes. *Science* 319(5868):1387–1391
7. Kuhlman B, Dantas G, Ireton GC, Varani G, Stoddard BL, Baker D (2003) Design of a

- 716 novel globular protein fold with atomic-level  
717 accuracy. *Science* 302(5649):1364–1368
- 718 8. Siegel JB, Smith AL, Poust S, Wargacki AJ,  
719 Bar-Even A, Louw C, Shen BW, Eiben CB,  
720 Tran HM, Noor E, Gallaheer JL, Bale J, Yoshi-  
721 kuni Y, Gelb MH, Keasling JD, Stoddard BL,  
722 Lidstrom ME, Baker D (2015) Computational  
723 protein design enables a novel one-carbon  
724 assimilation pathway. *Proc Natl Acad Sci U S*  
725 *A* 112(12):3704–3709
- 726 9. Ollikainen N, Kortemme T (2013) Computa-  
727 tional protein design quantifies structural con-  
728 straints on amino acid covariation. *PLoS*  
729 *Comput Biol* 9(11), e1003313
- 730 10. Fromer M, Linial M (2010) Exposing the co-  
731 adaptive potential of protein-protein interfaces  
732 through computational sequence design. *Bio-*  
733 *informatics* 26(18):2266–2272
- 734 11. McLaughlin RN, Poelwijk FJ, Raman A, Gosal  
735 WS, Ranganathan R (2012) The spatial archi-  
736 tecture of protein function and adaptation.  
737 *Nature* 491(7422):138–142
- 738 12. Schaefer C, Schlessinger A, Rost B (2010) Pro-  
739 tein secondary structure appears to be robust  
740 under in silico evolution while protein disorder  
741 appears not to be. *Bioinformatics* 26  
742 (5):625–631
- 743 13. Ollikainen N, Smith CA, Fraser JS, Kortemme  
744 T (2013) Flexible backbone sampling methods  
745 to model and design protein alternative con-  
746 formations. *Methods Enzymol* 523:61–85
- 747 14. Kellogg EH, Leaver-Fay A, Baker D (2011)  
748 Role of conformational sampling in computing  
749 mutation-induced changes in protein structure  
750 and stability. *Proteins* 79(3):830–838
- 751 15. Chiti F, Stefani M, Taddei N, Ramponi G,  
752 Dobson CM (2003) Rationalization of the  
753 effects of mutations on peptide and protein  
754 aggregation rates. *Nature* 424(6950):805–808
- 755 16. Smith CA, Kortemme T (2011) Predicting the  
756 tolerated sequences for proteins and protein  
757 interfaces using RosettaBackrub flexible back-  
758 bone design. *PLoS One* 6(7)
- 759 17. Harbury PB, Plecs JJ, Tidor B, Alber T, Kim PS  
760 (1998) High-resolution protein design with  
761 backbone freedom. *Science* 282  
762 (5393):1462–1467
- 763 18. Pokala N, Handel TM (2005) Energy func-  
764 tions for protein design: adjustment with  
765 protein-protein complex affinities, models for  
766 the unfolded state, and negative design of sol-  
767 ubility and specificity. *J Mol Biol* 347  
768 (1):203–227
- 769 19. Li Z, Yang Y, Zhan J, Dai L, Zhou Y (2013)  
770 Energy functions in de novo protein design:  
771 current challenges and future prospects. *Annu*  
772 *Rev Biophys* 42:315–335
20. Jacak R, Leaver-Fay A, Kuhlman B (2012) 773  
774 Computational protein design with explicit  
775 consideration of surface hydrophobic patches.  
776 *Proteins* 80(3):825–838
21. Bowie JU, Luthy R, Eisenberg D (1991) A 777  
778 method to identify protein sequences that  
779 fold into a known three-dimensional structure.  
780 *Science* 253(5016):164–170
22. Soding J (2005) Protein homology detection 781  
782 by HMM-HMM comparison. *Bioinformatics*  
783 21(7):951–960
23. Wu S, Zhang Y (2008) MUSTER: improving 784  
785 protein sequence profile-profile alignments by  
786 using multiple sources of structure informa-  
787 tion. *Proteins* 72(2):547–556
24. Zhang Y (2008) Progress and challenges in 788  
789 protein structure prediction. *Curr Opin Struct*  
790 *Biol* 18(3):342–348
25. Mitra P, Shultis D, Brender JR, Czajka J, Marsh 791  
792 D, Gray F, Cierpicki T, Zhang Y (2013) An  
793 evolution-based approach to de novo protein  
794 design and case study on *Mycobacterium*  
795 *tuberculosis*. *PLoS Comput Biol* 9(10),  
796 e1003298
26. Mitra P, Shultis D, Zhang Y (2013) EvoDe- 797  
798 sign: de novo protein design based on struc-  
799 tural and evolutionary profiles. *Nucleic Acids*  
800 *Res* 41(W1):W273–W280
27. Zhang Y, Skolnick J (2005) TM-align: a pro- 801  
802 tein structure alignment algorithm based on  
803 the TM-score. *Nucleic Acids Res* 33  
804 (7):2302–2309
28. Xu J, Zhang Y (2010) How significant is a 805  
806 protein structure similarity with TM-score  
807 = 0.5? *Bioinformatics* 26(7):889–895
29. Gribskov M, Homyak M, Edenfield J, Eisen- 808  
809 berg D (1988) Profile scanning for 3-  
810 dimensional structural patterns in protein  
811 sequences. *Comput Appl Biosci* 4(1):61–66
30. Gribskov M, Mclachlan AD, Eisenberg D 812  
813 (1987) Profile analysis – detection of distantly  
814 related proteins. *Proc Natl Acad Sci U S A* 84  
815 (13):4355–4358
31. Henikoff S, Henikoff JG (1992) Amino acid 816  
817 substitution matrices from protein blocks. *Proc*  
818 *Natl Acad Sci U S A* 89(22):10915–10919
32. Wu ST, Zhang Y (2008) ANGLOR: a compos- 819  
820 ite machine-learning algorithm for protein  
821 backbone torsion angle prediction. *PLoS One*  
822 3(10)
33. Chen HL, Zhou HX (2005) Prediction of sol- 823  
824 vent accessibility and sites of deleterious muta-  
825 tions from protein sequence. *Nucleic Acids Res*  
826 33(10):3193–3199
34. Faraggi E, Zhang T, Yang YD, Kurgan L, Zhou 827  
828 YQ (2012) SPINE X: improving protein sec-  
829 ondary structure prediction by multistep 829

- 830 learning coupled with prediction of solvent  
831 accessible surface area and backbone torsion  
832 angles. *J Comput Chem* 33(3):259–267
- 833 35. Schymkowitz J, Borg J, Stricher F, Nys R,  
834 Rousseau F, Serrano L (2005) The FoldX web  
835 server: an online force field. *Nucleic Acids Res*  
836 33(Web Server issue):382–388
- 837 36. Krivov GG, Shapovalov MV, Dunbrack RL  
838 (2009) Improved prediction of protein side-  
839 chain conformations with SCWRL4. *Proteins*  
840 77(4):778–795
- 841 37. Zhang Y, Skolnick J (2004) SPICKER: a clus-  
842 tering approach to identify near-native protein  
843 folds. *J Comput Chem* 25(6):865–871
- 844 38. Bazzoli A, Tettamanzi AGB, Zhang Y (2011)  
845 Computational protein design and large-scale  
846 assessment by I-TASSER structure assembly  
847 simulations. *J Mol Biol* 407(5):764–776
- 848 39. Brender JR, Zhang Y (2015) Recognizing  
849 mutations on protein-protein binding interac-  
850 tions through structure-based interface pro-  
851 files. *PLoS Comput Biol* (in press)
- 852 40. Mukherjee S, Zhang Y (2011) Protein-protein  
853 complex structure predictions by multimeric  
854 threading and template recombination. *Struc-  
855 ture* 19(7):955–966
- 856 41. Gao M, Skolnick J (2010) iAlign: a method for  
857 the structural comparison of protein-protein  
858 interfaces. *Bioinformatics* 26(18):2259–2265
- 859 42. Zhang Y (2012) [http://zhanglab.ccmb.med.  
860 umich.edu/PSSpred](http://zhanglab.ccmb.med.umich.edu/PSSpred)
- 861 43. Yang J, Yan R, Roy A, Xu D, Poisson J, Zhang  
862 Y (2015) The I-TASSER suite: protein struc-  
863 ture and function prediction. *Nat Methods* 12  
864 (1):7–8
- 865 44. Davis IW, Arendall WB, Richardson DC,  
866 Richardson JS (2006) The backrub motion:  
867 how protein backbone shrugs when a sidechain  
868 dances. *Structure* 14(2):265–274
- 869 45. Smith CA, Kortemme T (2008) Backrub-like  
870 backbone simulation recapitulates natural pro-  
871 tein conformational variability and improves  
872 mutant side-chain prediction. *J Mol Biol* 380  
873 (4):742–756
- 874 46. Roy A, Kucukural A, Zhang Y (2010) I-  
875 TASSER: a unified platform for automated  
876 protein structure and function prediction. *Nat  
877 Protoc* 5(4):725–738
- 878 47. Wu S, Skolnick J, Zhang Y (2007) Ab initio  
879 modeling of small proteins by iterative TAS-  
880 SER simulations. *BMC Biol* 5:17
- 881 48. Zhang Y (2007) Template-based modeling and  
882 free modeling by I-TASSER in CASP7. *Pro-  
883 teins* 69(S8):108–117
- 884 49. Zhang Y (2008) I-TASSER server for protein  
885 3D structure prediction. *BMC Bioinformatics*  
886 9:40
50. Kopp J, Bordoli L, Battey JN, Kiefer F, Schwede T (2007) Assessment of CASP7 predictions for template-based modeling targets. *Proteins* 69(Suppl 8):38–56
- 887 51. Cozzetto D, Kryshtafovych A, Fidelis K, Moul-  
888 J, Rost B, Tramontano A (2009) Evaluation of  
889 template-based models in CASP8 with stan-  
890 dard measures. *Proteins* 77(Suppl 9):18–28
- 891 52. Montelione GT (2012) Template based mod-  
892 eling assessment in CASP10. Paper presented  
893 at the 10th community wide experiment on the  
894 critical assessment of techniques for protein  
895 structure prediction, Gaeta, Italy, 9–12 Dec  
896 2012
- 897 53. Lee BK (2012) Template free modeling assess-  
898 ment in CASP10. Paper presented at the 10th  
899 community wide experiment on the critical  
900 assessment of techniques for protein structure  
901 prediction, Gaeta, Italy
- 902 54. Moul J, Pedersen JT, Judson R, Fidelis K  
903 (1995) A large-scale experiment to assess pro-  
904 tein structure prediction methods. *Proteins* 23  
905 (3):2–5
- 906 55. Moul J, Fidelis K, Kryshtafovych A, Rost B,  
907 Tramontano A (2009) Critical assessment of  
908 methods of protein structure prediction-  
909 round VIII. *Proteins Struct Funct Bioinf*  
910 77:1–4
- 911 56. Moul J (2005) A decade of CASP: progress,  
912 bottlenecks and prognosis in protein structure  
913 prediction. *Curr Opin Struct Biol* 15  
914 (3):285–289
- 915 57. Zhang Y (2008) I-TASSER server for protein  
916 3D structure prediction. *BMC Bioinformatics*  
917 9
- 918 58. Shultis D, Mitra P, Aslam N, Gray F, Piper C,  
919 Chinnaswamy K, Stuckey J, Cierpicki T, Wang  
920 S, Lei M, Zhang Y (2015) Redesigning the fold  
921 and binding specificity of BIR3 domain of X-  
922 linked inhibitor of apoptosis proteins using  
923 evolutionary profiles (submitted)
- 924 59. Rosano GL, Ceccarelli EA (2014) Recombi-  
925 nant protein expression in *Escherichia coli*:  
926 advances and challenges. *Front Microbiol*  
927 5:172
- 928 60. Prinz WA, Aslund F, Holmgren A, Beckwith J  
929 (1997) The role of the thioredoxin and glutar-  
930 edoxin pathways in reducing protein disulfide  
931 bonds in the *Escherichia coli* cytoplasm. *J Biol  
932 Chem* 272(25):15661–15667
- 933 61. Buchan JR, Stansfield I (2007) Halting a cellu-  
934 lar production line: responses to ribosomal  
935 pausing during translation. *Biol Cell* 99  
936 (9):475–487
- 937 62. Shultis D, Czajka J, Marsh D, Gray F, Brender  
938 JR, Mitra P, Cierpicki T, Zhang Y. Structural  
939 validation of computational protein designed  
940 through evolutionary methods (in preparation)

- 945 63. Baneyx F (1999) Recombinant protein expres- 992  
 946 sion in *Escherichia coli*. *Curr Opin Biotechnol* 993  
 947 10(5):411–421 994  
 948 64. Jana S, Deb JK (2005) Strategies for efficient 995  
 949 production of heterologous proteins in *Escher-* 996  
 950 *ichia coli*. *Appl Microbiol Biotechnol* 67 997  
 951 (3):289–298 998  
 952 65. Burgess RR (2009) Refolding solubilized 999  
 953 inclusion body proteins. *Methods Enzymol* 1000  
 954 463:259–282 1001  
 955 66. DelProposto J, Majmudar CY, Smith JL, 1002  
 956 Brown WC (2009) Mocr: a novel fusion tag 1003  
 957 for enhancing solubility that is compatible with 1004  
 958 structural biology applications. *Protein Expr* 1005  
 959 *Purif* 63(1):40–49 1006  
 960 67. Dantas G, Kuhlman B, Callender D, Wong M, 1007  
 961 Baker D (2003) A large scale test of computa- 1008  
 962 tional protein design: folding and stability of 1009  
 963 nine completely redesigned globular proteins. *J* 1010  
 964 *Mol Biol* 332(2):449–460 1011  
 965 68. Koga N, Tatsumi-Koga R, Liu GH, Xiao R, 1012  
 966 Acton TB, Montelione GT, Baker D (2012) 1013  
 967 Principles for designing ideal protein struc- 1014  
 968 tures. *Nature* 491(7423):222 1015  
 969 69. Socolich M, Lockless SW, Russ WP, Lee H, 1016  
 970 Gardner KH, Ranganathan R (2005) Evolu- 1017  
 971 tionary information for specifying a protein 1018  
 972 fold. *Nature* 437(7058):512–518 1019  
 973 70. Sreerama N, Woody RW (2000) Analysis of 1020  
 974 protein CD spectra: comparison of CONTIN, 1021  
 975 SELCON3, and CDSSTR methods in CDPro 1022  
 976 software. *Biophys J* 78(1):334 1023  
 977 71. Oberg KA, Ruyschaert JM, Goormaghtigh E 1024  
 978 (2004) The optimization of protein secondary 1025  
 979 structure determination with infrared and cir- 1026  
 980 cular dichroism spectra. *Eur J Biochem* 271 1027  
 981 (14):2937–2948 1028  
 982 72. Rehm T, Huber R, Holak TA (2002) Applica- 1029  
 983 tion of NMR in structural proteomics: screen- 1030  
 984 ing for proteins amenable to structural analysis. 1031  
 985 *Structure* 10(12):1613–1618 1032  
 986 73. Scheich C, Leitner D, Sievert V, Leidert M, 1033  
 987 Schlegel B, Simon B, Letunic I, Bussow K, 1034  
 988 Diehl A (2004) Fast identification of folded 1035  
 989 human protein domains expressed in *E. coli* 1036  
 990 suitable for structural analysis. *BMC Struct* 1037  
 991 *Biol* 4:4 1038
74. Hoffmann B, Eichmuller C, Steinhäuser O, 992  
 Konrat R (2005) Rapid assessment of protein 993  
 structural stability and fold validation via 994  
 NMR. *Methods Enzymol* 394:142 995  
 75. Schedlbauer A, Coudeyville N, Auer R, Kloiber 996  
 K, Tollinger M, Konrat R (2009) Autocorrela- 997  
 tion analysis of NOESY data provides residue 998  
 compactness for folded and unfolded proteins. 999  
*J Am Chem Soc* 131(17):6038 1000  
 76. Niesen FH, Berglund H, Vedadi M (2007) The 1001  
 use of differential scanning fluorimetry to 1002  
 detect ligand interactions that promote protein 1003  
 stability. *Nat Protoc* 2(9):2212–2221 1004  
 77. Pace CN, Scholtz JM (1997) Measuring the 1005  
 conformational stability of a protein. In: 1006  
 Creighton TE (ed) *Protein structure: a practi-* 1007  
*cal approach*. Oxford University Press, New 1008  
 York, NY, pp 299–321 1009  
 78. Shultis D, Dodge G, Zhang Y (2015) Crystal 1010  
 structure of designed PX domain from 1011  
 cytokine-independent survival kinase and 1012  
 implications on evolution-based protein engi- 1013  
 neering (submitted) 1014  
 79. Price WN 2nd, Chen Y, Handelman SK, Neely 1015  
 H, Manor P, Karlin R, Nair R, Liu J, Baran M, 1016  
 Everett J, Tong SN, Forouhar F, Swaminathan 1017  
 SS, Acton T, Xiao R, Luft JR, Lauricella A, 1018  
 DeTitta GT, Rost B, Montelione GT, Hunt 1019  
 JF (2009) Understanding the physical proper- 1020  
 ties that control protein crystallization by anal- 1021  
 ysis of large-scale experimental data. *Nat* 1022  
*Biotechnol* 27(1):51–57 1023  
 80. O’Hare B, Benesi AJ, Showalter SA (2009) 1024  
 Incorporating 1H chemical shift determination 1025  
 into 13C-direct detected spectroscopy of 1026  
 intrinsically disordered proteins in solution. *J* 1027  
*Magn Reson* 200(2):354–358 1028  
 81. Zhang Y, Hubner IA, Arakaki AK, Shakhno- 1029  
 vich E, Skolnick J (2006) On the origin and 1030  
 highly likely completeness of single-domain 1031  
 protein structures. *Proc Natl Acad Sci U S A* 1032  
 103(8):2605–2610 1033  
 82. Brylinski M, Gao M, Skolnick J (2011) Why 1034  
 not consider a spherical protein? Implications 1035  
 of backbone hydrogen bonding for protein 1036  
 structure and function. *Phys Chem Chem* 1037  
*Phys* 13(38):17044–17055 1038